Blind deconvolution using the Richardson–Lucy algorithm

Conference Paper *in* Proceedings of SPIE - The International Society for Optical Engineering · September 1994

DOI: 10.1117/12.197374

4 authors, including:

H. Lanteri
University of Nice Sophia Antipolis
115 PUBLICATIONS **970** CITATIONS

SEE PROFILE

Claude Aime
University of Nice Sophia Antipolis
213 PUBLICATIONS **2,234** CITATIONS

SEE PROFILE

Hubert Beaumont
Median Technologies
64 PUBLICATIONS **169** CITATIONS

SEE PROFILE

231238

Blind Deconvolution using the Richardson-Lucy Algorithm

Henri Lantéri, Claude Aime, Hubert Beaumont, and Philippe Gaucherel
Département d'Astrophysique. URA 709 du CNRS
Université de Nice Sophia-Antipolis. Parc Valrose 06108 Nice Cedex 2 France

ABSTRACT

The aim of this communication is to show how the Richardson-Lucy (RL) deconvolution algorithm can be applied to the blind deconvolution problem. After a brief description of the RL algorithm itself, we start with the basic papers of Ayers and Dainty(1988) and Lane (1992) and we introduce in their approach the RL algorithm in several different ways.

We show that the general behavior of the proposed method is analogous to that of the error-reduction algorithms and that good solutions can be obtained. The unregularized behavior of the RL algorithm is overcame by a limitation of the iteration number. Moreover we compare the structures of the various algorithms proposed here and emphasize the main differences.

The proposed algorithms are used to blindly deconvolve two types of objects (point-like and extended objects) blurred by simulated point spread functions similar to those observed at the focus of a small telescope in presence of atmospheric turbulence. The error reduction term is given as a function of the iteration number.

1. INTRODUCTION

The problem of blind deconvolution consist of seeking two unknown functions "g" and "h" knowing only "f" their convolution product, eventually affected by an additive noise "b". Using the concept of "zero sheets" Lane and Bates[1] have shown that it is possible to solve this problem, provided that g and h are of finite size and are functions of dimension higher or equal to 2.

We shall consider the problem of imaging an object through a turbulent medium, more precisely that of observation through the atmosphere with a small telescope. We shall denote g(x, y) the repartition of brightness for the object and h(x, y) the point spread function (PSF). We observe the intensity f(x,y) defined by the object image convolution relationship :

$$f(x,y) = h(x,y) * g(x,y) + b(x,y) \tag{1}$$

where b(x,y) is an additive signal independant noise. We emphasize that in the case of blind deconvolution, no reference point source is available to determine the PSF h(x, y). Recently Ayers and Dainty[2] proposed a blind deconvolution algorithm for the noise free case (b(x, y) = 0). This method was modified by Davey and al[3] and Seldin and Fienup[4] for specific applications. The structure of these algorithms closely look like those of the error reduction algorithm developed by Gerchberg and Saxton[5]. The "error" or cost function which is reduced in this algorithm can be written in the form

$$J = \int\int [f(x,y) - h(x,y) * g(x,y)]^2 \, dx \, dy \tag{2}$$

The Ayers Dainty algorithm alternates between the object domain and the Fourier domain, enforcing known constraints in both domains. The object constraints are mainly a positivity constraint and in some cases, a support constraint. This algorithm is summarized in Fig. 1, where we can observe that two deconvolutions by inverse or Wiener filtering are applied at each global iteration. The algorithm is started with an initial estimate of one of the two functions (here h_0).

In more recent works, Mc. Callum[6] used the simulated annealing method for minimization of composite functional which includes the constraints. Recently, Lane[7] developed a similar approach using the conjugate gradient method. In the work we present here, we use Richardson[8] - Lucy[9]'s iterative deconvolution algorithm in the Ayers - Dainty's general configuration instead of the inverse filtering, then we suggest several developments of the method.

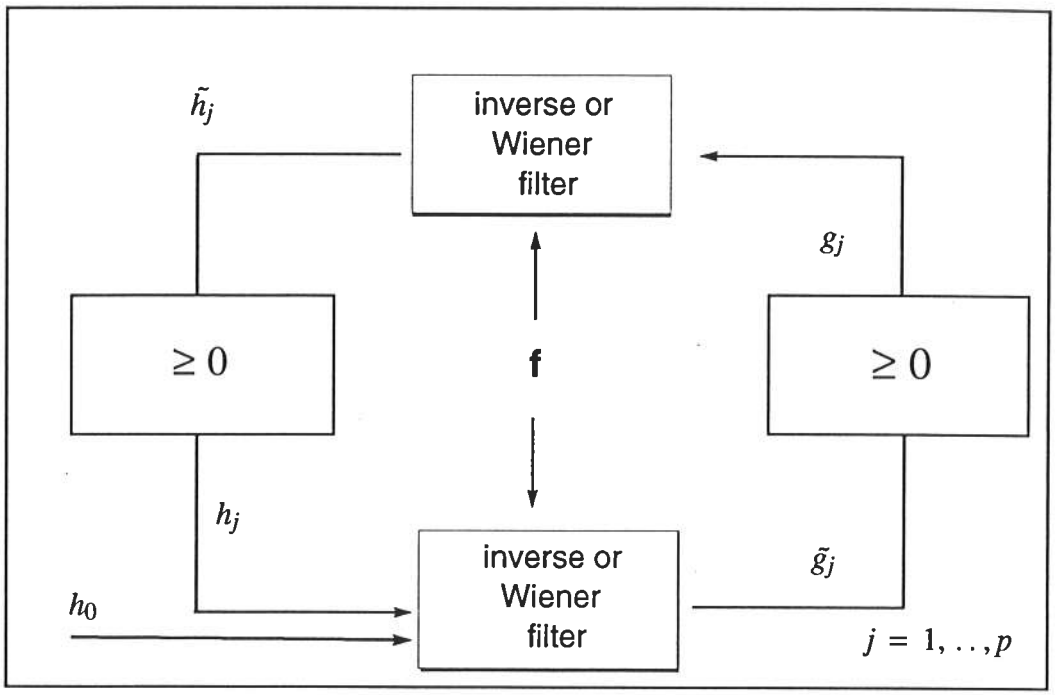

Figure 1. Schematic representation of the blind deconvolution technique proposed by Ayers and Dainty[2]. As described in the body of the paper, f is the measurement, h and g are the unknown.

2. THE RICHARDSON - LUCY ALGORITHM

The RL algorithm has been extensively used for image reconstruction in astrophysics and in nuclear medicine; it was derived from Bayesian considerations and can be summarized by the following iterative relation, where the PSF h(x,y) is assumed to be known and normalized :

$$g_o(x,y) = C^{ste} \tag{3}$$

$$g_{k+1}(x,y) = g_k(x,y) \cdot h^*(-x,-y) * \frac{f(x,y)}{h(x,y) * g_k(x,y)} \tag{4}$$

With a constant initial guess $g_0(x,y)$, positive and normalized, this algorithm leads to successive estimates $g_k(x,y)$ which are implicitly positive. In more recent works, Shepp and Vardi[10] have shown that the previous iterative relations could be obtained making the assumption of a Poisson process in image formation. In this case the search of the maximum of the likelihood P(f/g) using the Expectation - Maximisation method, as proposed by Dempster and al[11], leads to the relation reported by Richardson and Lucy.

Due to the ill - posedness nature of the problem, we can observe large fluctuations of the solutions as the number of iteration increases. This is caused by the lack of constraints on the smoothness of the solution. We can avoid this drawback either introducing a smoothness constraint using Bayes theorem and maximizing the probability a posteriori P(g/f), or in an empirical way by limiting the number of iterations in the RL algorithm. Llacer and Nunez[12] have developed similar considerations in a recent work. Regarding the present contribution, we use the unregularized algorithm (relations 3 and 4), and we stop the iterations before instabilities appear.

3. BLIND DECONVOLUTION ALGORITHMS

The basic modification of the Ayers Dainty (AD) algorithm we propose here consists of substituting the Wiener filter[3] (or the inverse filter[2]) by an iterative deconvolution using the RL algorithm. So doing, it is no more necessary to apply the

positivity constraint using orthogonal projections. This algorithm is described in Fig. 2 and Fig. 3.

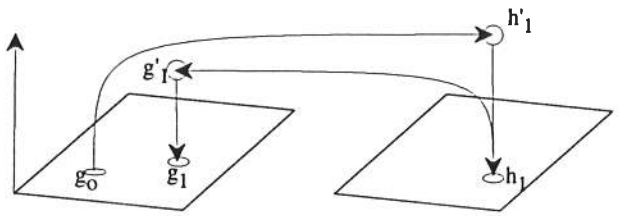

(Ayers Dainty)

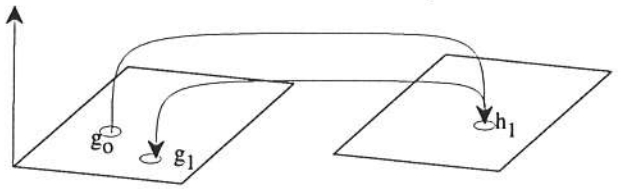

(Richardson Lucy)

Figure 2. Schematic representation of the Ayers Dainty (AD) blind deconvolution algorithm and of the modification induced by the use of the Richardson Lucy (RL) algorithm. The horizontal planes represent positive functions. In the AD scheme, the first guess g_0 leads to a function h'_1 that is the exact deconvolved quantity of f by g_0, but that presents unwanted negative parts. The application of positivity constraint gives the projection of h'_1 in h_1. This function is later used to deconvolve f to obtain g'_1, and so on. In the new algorithm we propose, the RL deconvolution procedure keeps the functions in the positive surfaces. The new function h_1 is the best deconvoluted function - in the RL sense - of g_0; note that the h_1 in the two schemes are different.

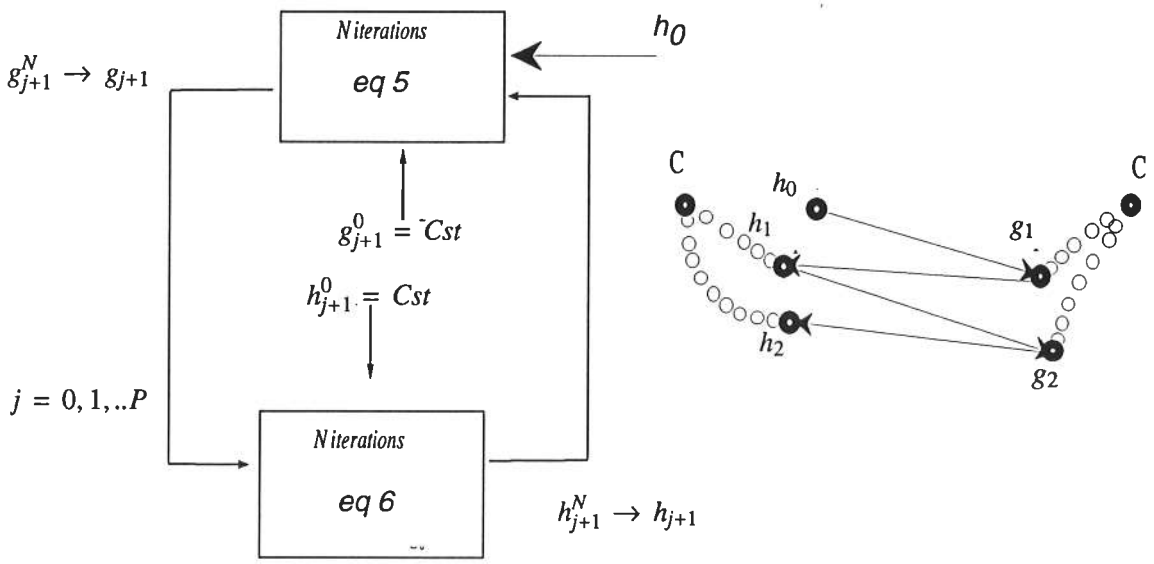

Figure 3. Schematic representations of the modified AD algorithm using the RL deconvolution technique. Each outer loop contains two inner iterative RL sequences. The two representations show that h_0 only is necessary to start the general procedure. Each RL sequence starts from an initial estimate that is a constant. In a more formal way, if we denote u_j^k the

estimate of a function "u" for the k^{th} iteration in the RL algorithm of the j^{th} loop of the global scheme, we can describe the iterative process using the following relations:

$$
\begin{aligned}
& h_O \ (guess) \\
& j = 0, 1, \ldots P \\
& \quad g_{j+1}^{0} = C^{ste} \\
& \quad k = 0, 1, \ldots N \\
& \quad g_{j+1}^{k+1} = g_{j+1}^{k} \cdot h_j^{*}(-x,-y) * \frac{f(x,y)}{h_j(x,y) * g_{j+1}^{k}(x,y)} \qquad (5) \\
& \quad g_{j+1}^{N} \rightarrow g_{j+1} \\
& \quad h_{j+1}^{0} = C^{ste} \\
& \quad k = 0, 1, \ldots N \\
& \quad h_{j+1}^{k+1} = h_{j+1}^{k} \cdot g_{j+1}^{*}(-x,-y) * \frac{f(x,y)}{g_{j+1}(x,y) * h_{j+1}^{k}(x,y)} \qquad (6) \\
& \quad h_{j+1}^{N} \rightarrow h_{j+1}
\end{aligned}
$$

This algorithm has been implemented to deconvolve an extended object (the letter F) convolved by a simulated PSF corresponding to the observation with a little telescope in presence of atmospheric turbulence as shown in Fig(4).

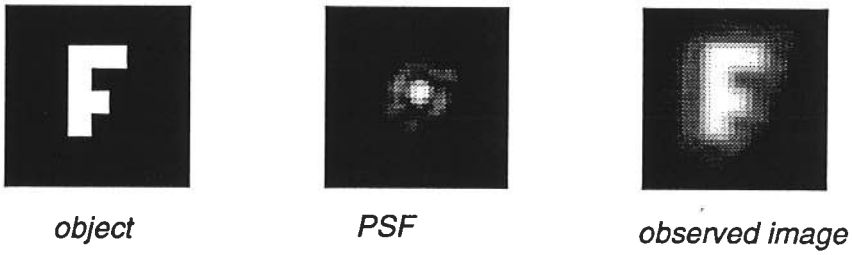

Figure 4. The observed image is the convolution of the object (the letter F) by the PSF (no added noise).

The results we obtained are shown in Fig. (5B) for N = 20 and P = 50; one can note the reasonable aspect of the results. The error is drawn in an logarithmic scale in Fig(5A) ; it presents a global, but not monotonous, decrease.

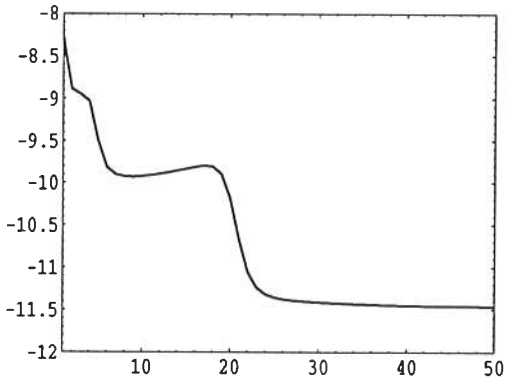

Figure 5A. Representation in a log-lin scale of the error, or cost function, as described by relation (2) as a function of the outer iteration number of the blind deconvolution algorithm (Fig. 3) . The inner iteration number for the RL deconvolution was 20. The cost function surprisingly increases after 10 iterations and decreases afterwards.

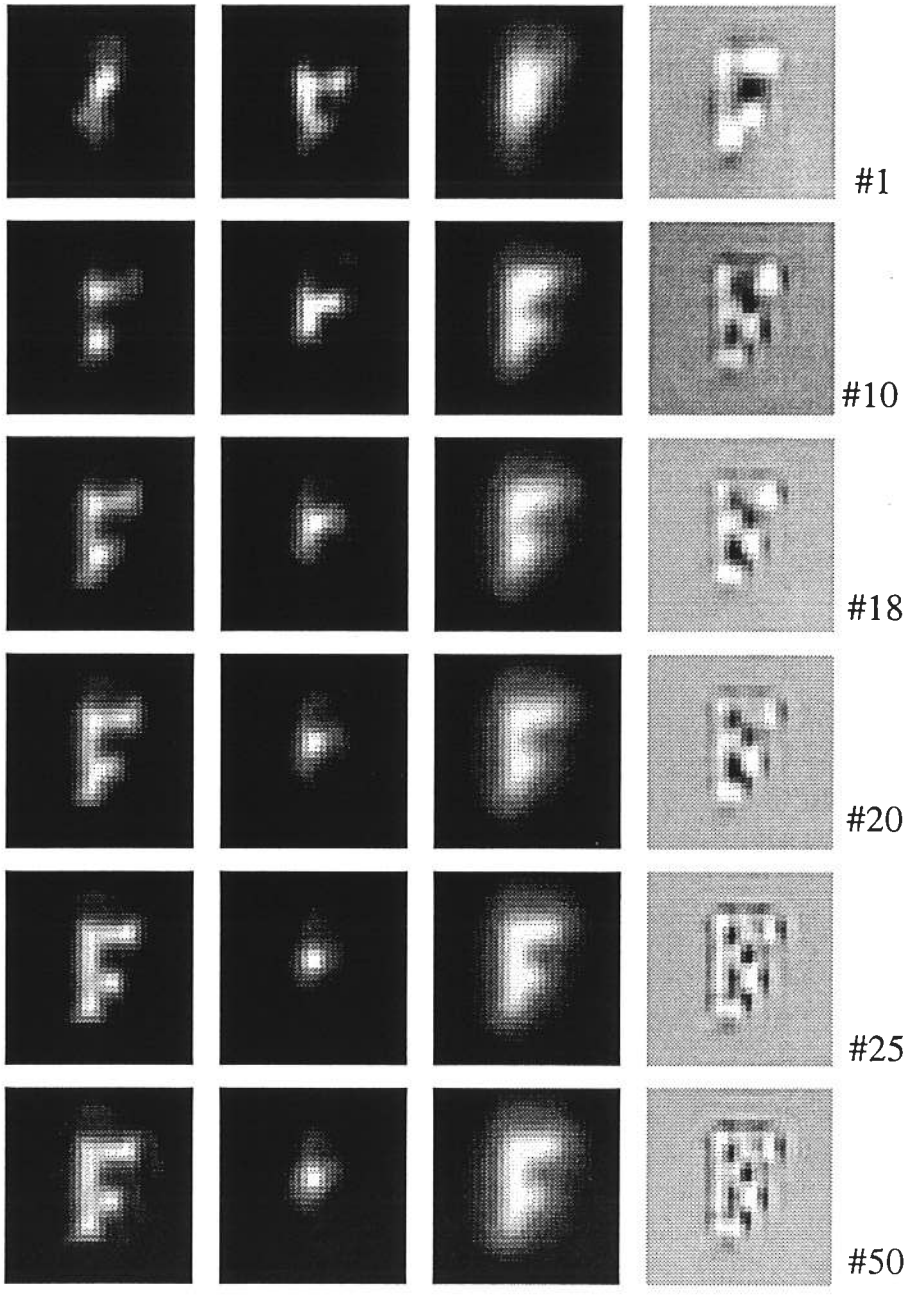

Figure 5 B. Blind deconvolution using the algorithm defined by relations (5) and (6) and illustrated in Fig.(3). We have plotted the reconstructed images at various steps (from #1 to #50) of the outer loop : estimated object (a) and PSF (b); their convolution product (c), to be compared with the observed image shown in Fig 4. The last column (d) represents the difference point to point between (c) and the observed image.

In order to enhance the speed of convergence one may intend to substitute the constant initial guess of each RL sequence with the estimate resulting from the previous iterations, that is :

$$h^{0}_{j+1} = h_j$$
$$g^{0}_{j+1} = g_j \qquad (7)$$

However, this procedure has not given satisfactory results in this example.The second configuration we used consists of performing one single step of the RL algorithm in each global loop. That is what is depicted in Fig (6) and can be expressed using the following relations:

$$h_0\,(\text{guess}) \;,\; g_0 = C^{ste}$$

$$j = 0, 1, \ldots P$$

$$g_{j+1}(x,y) = g_j(x,y) \cdot h_j^*(-x,-y) * \frac{f(x,y)}{h_j(x,y) * g_j(x,y)} \qquad (8)$$

$$h_{j+1}(x,y) = h_j(x,y) \cdot g_{j+1}^*(-x,-y) * \frac{f(x,y)}{g_{j+1}(x,y) * h_j(x,y)} \qquad (9)$$

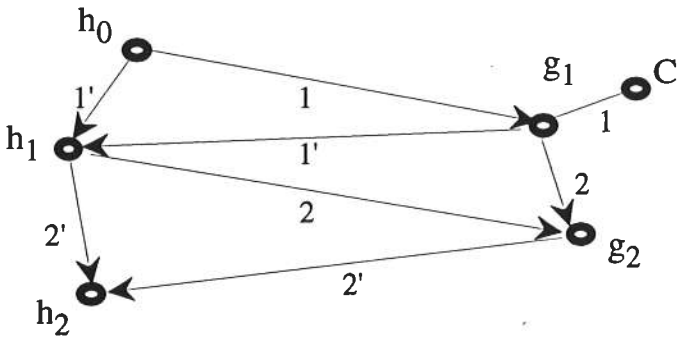

Figure 6. Modified version of the blind deconvolution algorithm (relations 8 and 9). The RL algorithm is used in a single step manner and the result of the deconvolution for the PSF is used to derive the estimated object, and reciprocaly.

This algorithm was implemented for the case specified in Fig (7A). We can notice that the object and the P.S.F are properly obtained after only 50 global loops (Fig. 7B) and the error curve regularly decreases (Fig. 7C).

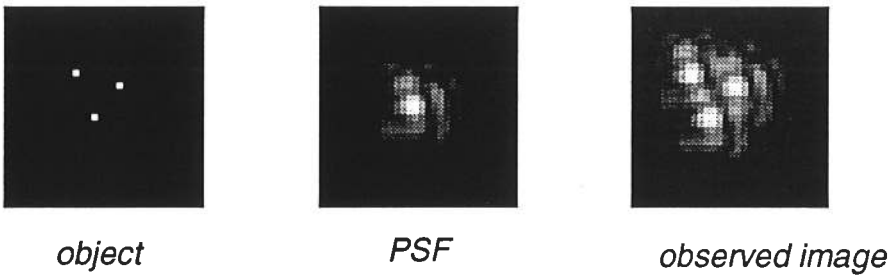

Figure 7A. The object is made of 3 points. The observed image is the convolution of the object by the PSF in a similar way as the images shown in Fig.4. No noise was added to the observed image.

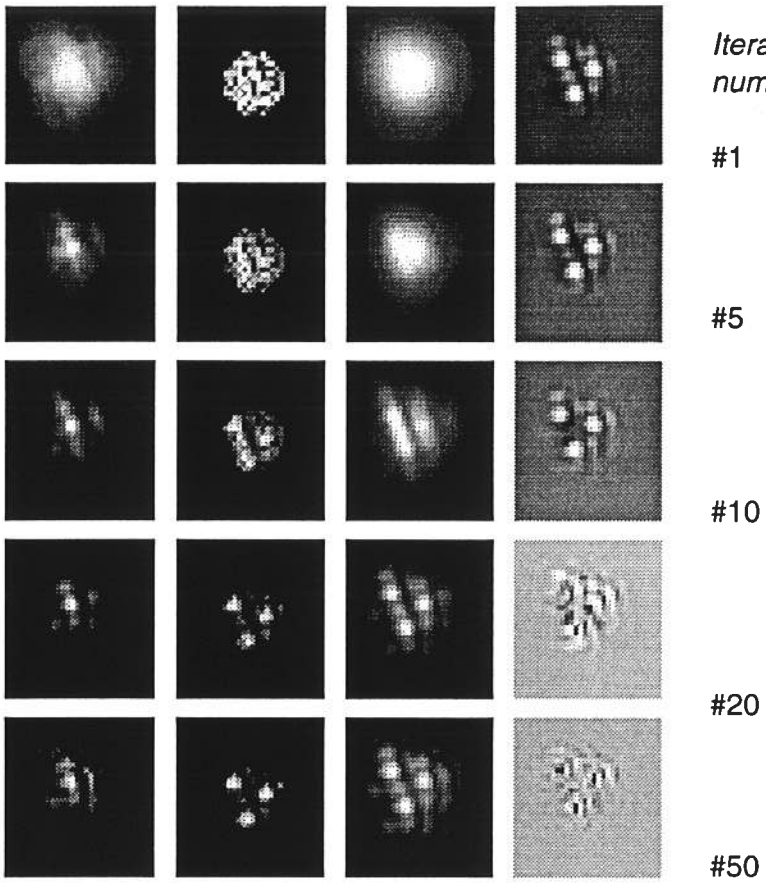

Figure 7 B. Reconstructed images at various steps (from #1 to #50) of the iteration described by Fig. 6 and relations (8) and (9); estimated PSF (a) and object (b); their convolution product (c), to be compared with the observed image shown in Fig 7A. The last column (d) represents the difference between (c) and the observed image.

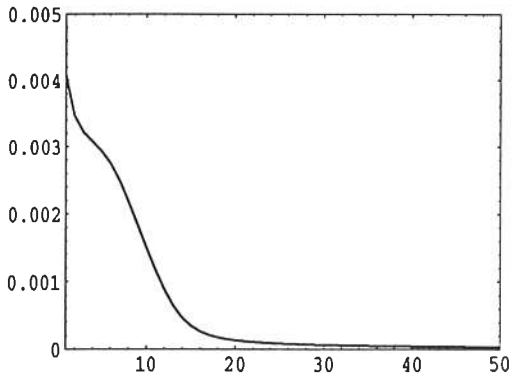

Figure 7 C. Error, or cost function, as described by relation (2) as a function of the iteration number of the blind deconvolution algorithm (Fig. 3) represented in a linear scale.

However these results strongly depend on the processed object. This fact can be put in evidence if the algorithm is used to process the data of Fig. (4). We can observe in Fig.(8A) that even for a very large number of iterations (up to 3000) and although a significant decrease of the error (Fig. 8B), the solutions obtained are unsatisfactory. It seems to indicate that the error function used is irrelevant regarding the quality of the results.

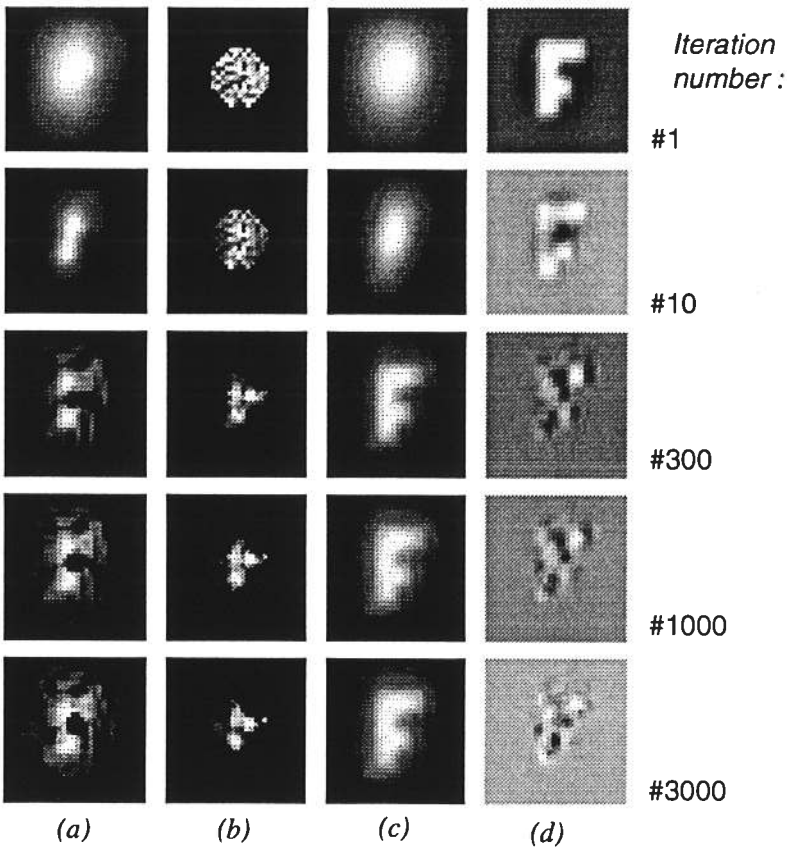

Figure 8 A. Reconstructed images at various steps (from #1 to #3000) of the iteration with no inner do loop (see Fig. 6 and relations 8 and 9) ; estimated object (a) and PSF (b); their convolution product (c), to be compared with the observed image shown in Fig 4. The last column (d) represents the difference point to point between (c) and the observed image. In that case the solution is not satisfactory.

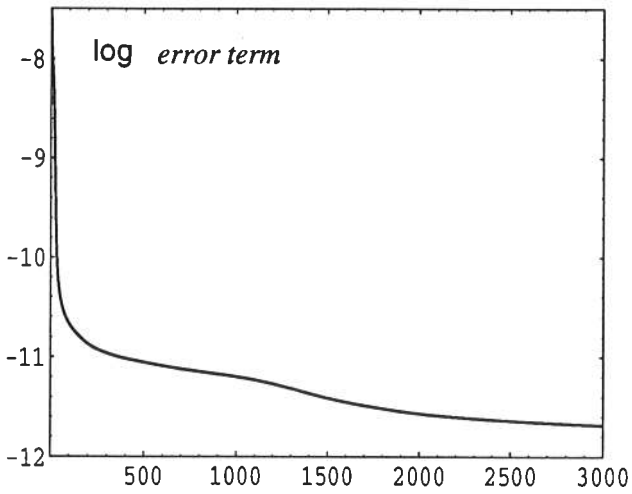

Figure 8 B. Error, or cost function, as described by relation (2) as a function of the iteration number of the blind deconvolution algorithm (Fig. 3) represented in a logarithmic scale. The rather low value obtained for the error only indicates that the convolution of reconstructed object and PSF gives a good approximation of the observation, as it can be seen in above Fig. 8 (c and #3000), but that is not enough to secure a good result.

In the last variant of the algorithm similar to that suggested by Holmes[13] we have computed in the same time h(x,y) and g(x,y) of the j + 1 iteration from the estimates of the j th iteration, as represented in Fig. (9). When applied to the data of Fig.(4).

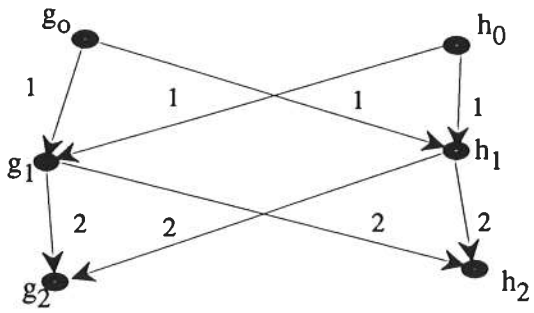

Figure 9. Schematic representation of the algorithm corresponding to relations (10) and (11)

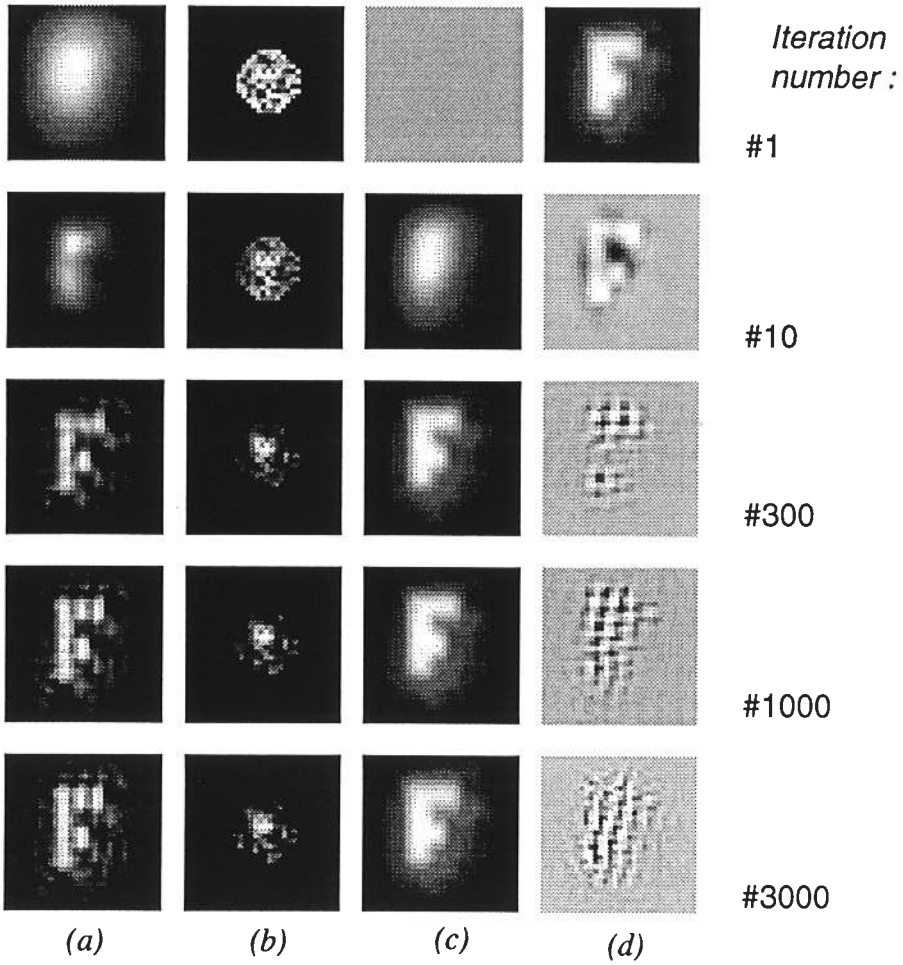

Figure 10 A. Reconstructed images at various steps (from #1 to #3000) of the iteration with no inner do loop (see Fig. 9 and relations 10 and 11) ; estimated object (a) and PSF (b); their convolution product (c), to be compared with the observed image shown in Fig 4. The last column (d) represents the difference point to point between (c) and the observed image. This computation give a much better solution than that obtained in Fig.8. The speckled appearance of the result is probably an effect of the unregularized nature of the blind deconvolution we have performed and could be improved by applying some kind of smoothness constraints.

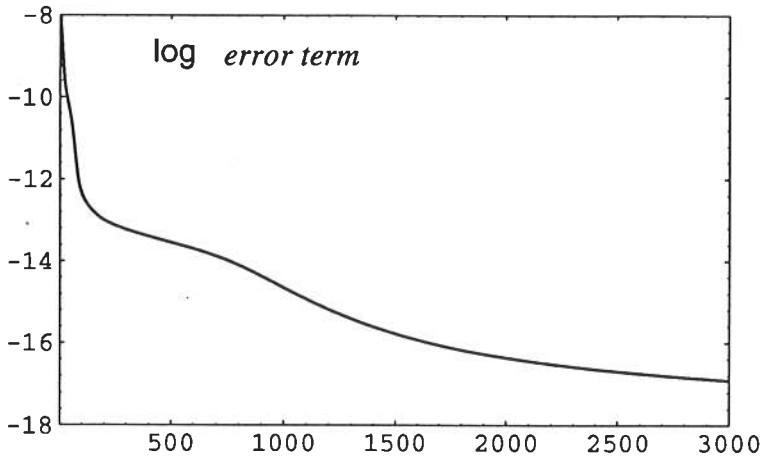

Figure 10 B. Error term of the reconstruction shown in Fig 10 A.

This algorithm can be expressed by the following relations :

$$h_0\,(guess{:}see\,fig10A\;a\text{-}\#1)\,,\; g^{o}_{j+1} = C_{ste}$$

$$j = 0, 1, ..p$$

$$h_{j+1}(x,y) = h_j(x,y) \cdot g_j^*(-x,-y) * \frac{f(x,y)}{g_j(x,y) * h_j(x,y)} \tag{10}$$

$$g_{j+1}(x,y) = g_j(x,y) \cdot h_j^*(-x,-y) * \frac{f(x,y)}{h_j(x,y) * g_j(x,y)} \tag{11}$$

Obviously in this method the initial guess have to be different. The results obtained are depicted in Fig.(10A) and the corresponding error is depicted in Fig.(10B). We still note here the goodness of the result considering the few constraints used. The error is clearly lower than in the other cases even though this seems not to be connected with the visual quality of the images.

4. CONCLUSION

We have shown that the use of the algorithm of Richardson and Lucy in the blind deconvolution configuration proposed by Ayers and Dainty is of interest for image reconstruction and can lead to good results, at least for the two kinds of images (point-like and extended objects) and point spread functions we have processed here. We have proposed several ways for doing the blind deconvolution, mostly depending upon the number of iterations and first guess of the RL algorithm.

We would like to emphasize how much it is essential to exactly specify how the iterations have been made. This remark would equally apply if a classical iterative gradient algorithm was used instead of the RL algorithm. In a more general way in any optimization attempt it is important to specify :

- what are the constraints ?
- how can them be expressed ?
- what strategy can be applied to solve a non linear minimization problem under constraints?

In any case the use of an error reduction algorithm is only one element in solving this problem. The main difficulty is probably less the choice of an algorithm than the way in which the problem can be expressed.

5. REFERENCES

1. R. G. Lane and R. H. T. Bates, " Automatic Multidimensional Deconvolution," J.Opt.Soc.Am. A, Vol. 4, pp. 180 - 188, 1987.

2. G. R. Ayers and J. C. Dainty "Iterative Blind Deconvolution Method and it's Application," Optics Letters, Vol. 13, pp. 547 - 549, 1988.

3. B. L. K. Davey, R. G. Lane and R. H.T. Bates "Blind Deconvolution of Noisy Complex-Valued Images," Optics Comm., Vol. 69, pp. 353 - 356, 1990.

4. J. H. Seldin and J. R. Fienup "Iterative Blind Deconvolution Algorithm Applied to Phase Retrieval," J.Opt.Soc.Am. A, Vol. 7, pp. 428 - 433, 1990.

5 R. W. Gerchberg and W. O. Saxton "A Practical algorithm for the determination of phase from image and diffraction plane pictures," Optik,Vol. 35, pp. 237-246, 1972.

6 B. C. Mc. Callum "Blind Deconvolution by Simulated annealing," Optics Comm.,Vol. 75 , pp. 101 - 105, 1990.

7. R. G. Lane " Blind Deconvolution of Speckle Images" J.Opt.Soc.Am. A,Vol.9, pp. 1508 - 1514, 1992.

8. W. H. Richardson "Bayesian Based Iterative Method for Image Restoration," J.Opt.Soc.Am.,Vol. 62, pp. 55 - 59, 1972.

9. L. B. Lucy " An Iterative Technique for the Rectification of Observed Distributions," Astronl J.,Vol. 79, pp. 745 - 754, 1974.

10. L. A. Shepp and Y. Vardi "Maximum Likelihood Reconstruction for emission Tomography," IEEE Trans. MED Imaging,Vol. MI - 1, pp. 113 - 122, 1982.

11. A. P. Dempster, N. M. Laird and D. B. Rubin "Maximum Likelihood from Incomplete Data via the E.M. Algorithm," J. Roy. Stat. Soc.,Vol. 39, pp. 1 - 38, 1977.

12. J. Llacer and J. Nunez "Iterative Maximum Likelihood Estimator and Bayesian Algorithm for Image Reconstruction in Astronomy," Proc. workshop on the restoration of H.S.T images and spectra (Baltimore - Md), pp. 62 - 69, 1990.

13 T. J. Holmes "Blind Deconvolution of Quantum - Limited Incoherent Imagery: Maximum Likelihood Approach." J.Opt.Soc.Am. A, Vol. 9, pp.1052 - 1061. (1992).